Pure Appl. Chem., Vol. 81, No. 12, pp. 2327–2335, 2009.
doi:10.1351/PAC-CON-08-11-23
© 2009 IUPAC, Publication date (Web): 18 November 2009

Photocatalytic degradation of methylene blue on magnetically separable FePc/Fe_3O_4 nanocomposite under visible irradiation*

Kun Wang‡, Lixia Yu, Sheng Yin, Henan Li, and Huaming Li

College of Chemistry and Chemical Engineering, Jiangsu University, 301 Xuefu Road, Zhenjiang, 212013, China

Abstract: A novel magnetically separable photocatalyst iron phthalocyanine/Fe_3O_4 (FePc/Fe_3O_4) nanocomposite was easily prepared by an organic–inorganic complexation technique, and characterized by transmission electron microscopy (TEM), X-ray powder diffraction (XRD), and Fourier transform-infrared (FTIR). This functional nanocomposite has been found to exhibit high catalytic activity in the presence of added hydrogen peroxide, for oxidative degradation of methylene blue (MB) under visible light irradiation. Under these conditions, MB (10 mg/l) underwent about 78 % oxidation in 2 h, and the catalyst still retained high activity after five catalytic cycles. Intervening recovery was easily achieved by changing the external magnetic field.

Keywords: iron phthalocyanine; magnetically separable; photocatalysis; nanocomposite; repetitive use; visible light.

INTRODUCTION

The development of facile, cheap, and green methods for treatment of organic pollutants has been a focal subject in the field of environmental science and technology. Among many strategies including physical, chemical, biological, and photocatalytic methods, photocatalysis is a promising technology for the treatment of contaminants due to its potential use of sunlight as the energy source to degrade organic pollutants [1–3]. During the past 20 years, many photoexcitable inorganic semiconductors have been used as photocatalysts to decompose or destroy the organic pollutants [4–10]. However, due to their large band-gap energy, the absorption band of these inorganic semiconductors is deep in the UV region and very low in the visible light region, limiting the practical application of natural solar light [4]. While some improved strategies have been adopted by the preparation of doped inorganic semiconductors to increase their absorption in the visible light region [5–10], the photocatalytic activity of the resulting semiconductor may still need improvement [10].

Organic dyes have the attractive advantages of possessing high molar absorptivity in the visible region and match the light source emission spectrum with solar light [10]. Metallophthalocyanines (MPcs) are not only a family of well-known classical dyes, but also advanced materials used in photovoltaic, nonlinear optical, solar cell, catalyst, and sensor field, and so on, because of their unique physical and chemical property combined with nontoxicity and low cost [11–13]. Especially, their excellent physicochemical properties, including strong absorption in the visible region, make them a strong can-

---

*Paper based on a presentation at the International Symposium on Novel Materials and their Synthesis (NMS-IV) and the 18th International Symposium on Fine Chemistry and Functional Polymers (FCFP-XVIII), 15–18 October 2008, Zhenjiang, China. Other presentations are published in this issue, pp. 2253–2424.

‡Corresponding author: E-mail: wangkun@ujs.edu.cn

didate for application in the photocatalytic degradation of organic pollutants [14–16], such as FePcS, and were applied to the oxidative degradation of organic pollutants [15] and the photooxidation of cyclohexene catalyzed by zinc phthalocyanine in the organic system [16]. However, these reactions noted above are conducted in a homogeneous aqueous medium or organic system, which bring about the disadvantages of the secondary contamination, catalyst separation, and repetitive use. Therefore, studies of the related catalyst immobilization have been carried out by immobilizing MPcs onto various substrates such as zeolite-X [10], layered double hydroxides [17], cellulosic fiber [18], or inorganic oxide particles [19–21]. While this approach provided a solution to the solid–liquid separation problem, using cross-flow filtration and centrifugation is still a problem for the practical application.

As an alternative strategy, some core-shell structured and magnetic functionalized materials have been used as the photocatalysts in the field of oxidative degradation of organic pollutants, due to their segregative property from the reaction system by an external magnetic field [22–27], and these magnetic photocatalysts were fabricated using the magnetic granule and photoactive material as the core and shell, respectively. For example, Misra et al. [22,23] prepared titania-coated nickel ferrite and found that the composite can be applied as a removable antimicrobial photocatalyst; Ao et al. [27] found the photocatalyst, titania-coated γ-Fe_2O_3 magnetic activated carbon, can be separated easily by an external magnetic field, and the degradation rate of phenol was still over 80 % after six repetitive uses. Although some core-shell structured magnetic photocatalysts have received much more attention, there is little research on the magnetic MPc composites used as photocatalysts, which can photodegrade organic pollutants in the visible light region without any adulterant.

Our work concerns fabricating the core-shell magnetic photocatalyst with photocatalytic activity in the visible region, facile separation from the reaction system and high recycling activity. So, iron(III) phthalocyanine (FePc) was selected as the model compound of MPcs, which was used as photocatalyst shell and which possesses strong absorption in the visible region, and Fe_3O_4 magnetic nanoparticle was selected as the photocatalyst core, which has high surface areas and supermagnetism. In the present work, we fabricated iron(III) phthalocyanine/Fe_3O_4 (FePc/Fe_3O_4) nanocomposite by the organic–inorganic complex technique, and methylene blue (MB), which is one of the thiazine dyes and is hard to degrade, was selected as the model object of photocatalytic degradation. The resulting materials were characterized by X-ray diffraction (XRD), Fourier transform-infrared (FT-IR), transmission electron microscopy (TEM), and the photocatalytic activity of FePc/Fe_3O_4 for MB degradation in aqueous solution was tested.

EXPERIMENTAL

Reagents and apparatus

FePc was purchased from Fluka; other reagents were purchased from Shanghai Reagent Corporation (Shanghai, China) and used as received without further purification.

The XRD analysis was conducted on a Bruker D8 diffractometer with high-intensity Cu Kα (λ = 1.54 Å). TEM images were obtained from micrographs and selected-area electron diffraction. The UV–vis diffuse reflectance spectrum of the sample was measured by a UV–vis spectrometer. The IR spectra of the samples were obtained from FT-IR Spectrometer (Nicolet Nexus 470 FT-IR).

Fabrication of FePc/Fe_3O_4 nanocomposite

Fe_3O_4 nanoparticles were prepared by a chemical coprecipitation principle and technique [28]. The water absorbed in the surface of Fe_3O_4 nanoparticles was removed as completely as possible using a phase-transfer method [29]. FePc/Fe_3O_4 nanocomposite was prepared by the organic–inorganic complex technique: briefly, the Fe_3O_4 nanoparticles were transferred into suitable organic solvent, then the solution of FePc was added and the mixture was stirred. After this mixture was evaporated in vacuum at certain temperature, the FePc/Fe_3O_4 nanocomposites were formed.

The proportion of FePc in this composite is about 10 %, which was tested as follows: the dried solid particles were dissolved in the HCl to dissolve Fe_3O_4 nanoparticles, the precipitate left was the FePc packed on the surface of Fe_3O_4 nanoparticles, and then the weight components of FePc were obtained.

Photocatalytic experimental

Photocatalytic activities of FePc/Fe_3O_4 nanocomposite samples were evaluated by photocatalytic oxidation of MB under visible light irradiation. A 200-W incandescent lamp was used as light source. A UV cut-filter, which can filter out UV light with wavelengths below 420 nm, was placed between the glass tube and the lamp. Before the illumination, catalyst (0.05 g) was added to MB (50 ml, 10 mg/l), and nitrogen was passed through the solution for 30 min in the dark, in order to establish MB absorption–desorption equilibrium prior to commencement of the photocatalytic reaction. All the experiments that follow were carried out after the solution reached the absorption–desorption equilibrium, and after adding 1 ml H_2O_2 (9 M) into the system, and then the incandescent lamps were opened. In the repetitive use experiment of the catalyst, an NdFeB strong magnet (20 ↔ 20 ↔ 5 mm) was used as an external magnetic field. When one reaction was finished, the magnet was placed under the glass tube; and then the FePc/Fe_3O_4 nanocomposite was isolated from the solution; finally, the obtained sedimentation was washed with distilled water several times and dried in a vacuum oven at room temperature for the next use.

The degradation efficiency of MB was analyzed by UV–vis spectroscopy at intervals. According to the Beer–Lambert law [30], the concentration of MB is proportional to absorbance of MB, so the oxidation efficiency of MB can be calculated by $R = \frac{C_0 - C}{C_0} \times 100\,\% = \frac{A_0 - A}{A_0} \times 100\,\%$, where A_0, A, and C_0, C are the absorbance and concentration of MB when reaction time is 0 and t, respectively. And the oxidation efficiency of MB can be also calculated by $R = C/C_0$ intuitively.

RESULTS AND DISCUSSION

Characterization of Fe(III)Pc/Fe_3O_4 nanocomposite

XRD patterns of the prepared samples are presented in Fig. 1. Figure 1a shows the XRD pattern of the Fe_3O_4 MNPs. The main diffraction peaks at 220, 311, 400, 422, 511, 400° were identical to the standard cubic spinel structure of Fe_3O_4 MNPs cards (JCPDS 65-3107), and no other crystalline phases were observed in the XRD diffractogram. The crystal lattice parameters were calculated as follows: $a = 8.67784$ Å, $b = 6.72058$ Å, $c = 6.5101$ Å. Similar characteristic peaks can also be found in Fig. 2b, suggesting that the crystalline structure of Fe_3O_4 MNPs did not change through the modification with FePc.

MPcs have emblematical absorption at 750, 880, 950, 1050, 1090, 1120 cm^{-1}, which can be see from Figs. 2a and 2b. The FT-IR spectrum of MPcs immobilized onto solid substrates is somewhat different from that of MPcs, and their FT-IR bands were broadened in the 1500–1700 cm^{-1} region, perhaps due to changes in molecular geometry and lowered symmetry of Pc moiety on solid substrates [31].

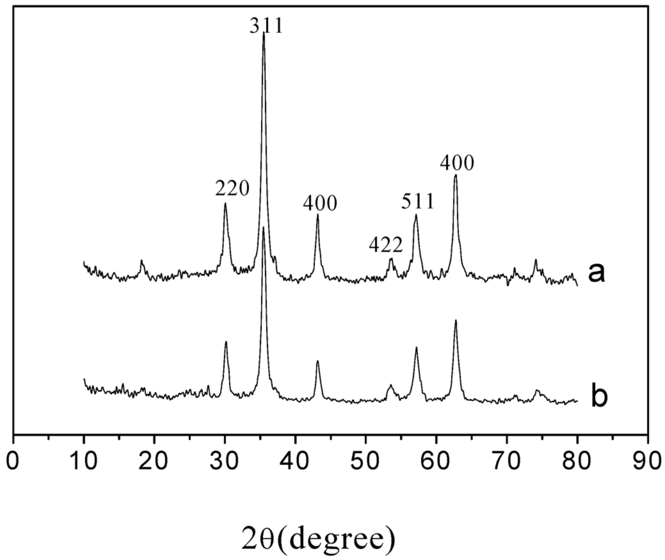

Fig. 1 XRD patterns of (a) Fe_3O_4 nanoparticles and (b) FePc/Fe_3O_4 nanocomposites.

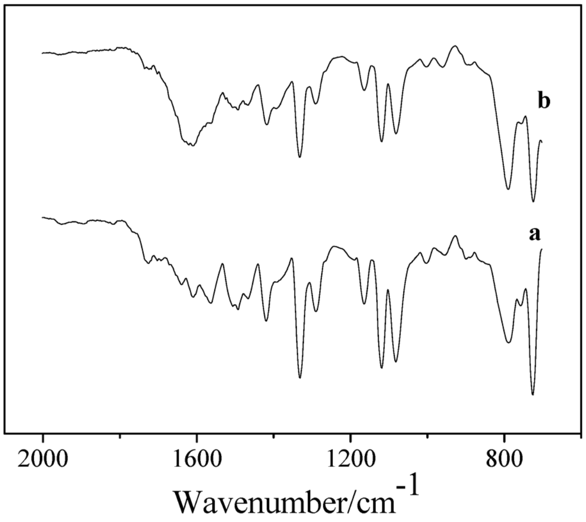

Fig. 2 FT-IR spectra of (a) FePc and (b) FePc/Fe_3O_4 nanocomposite.

Figure 3a is the TEM image of the prepared Fe_3O_4 nanoparticles, which shows that a slight particle agglomeration was clearly observed for the unmodified nanoparticles, and the primary particle size is likely closer to 10 nm in diameter. After FePc was coated onto the surface of Fe_3O_4 nanoparticles (Fig. 3b), the aggregation of the nanoparticles was reduced. Additionally, the shape and size of the composite did not change obviously. It was still close to 10 nm with spherical shape. Though after three times use for photocatalytic test, the compound is somewhat aggregate (Fig. 3c), and it still can be seen that the compound maintains primary shape and size. As a result, it can be kept for further application in the photocatalytic oxidation. Furthermore, the efficiency of this catalyst in the following work, confirmed additionally by its practical value.

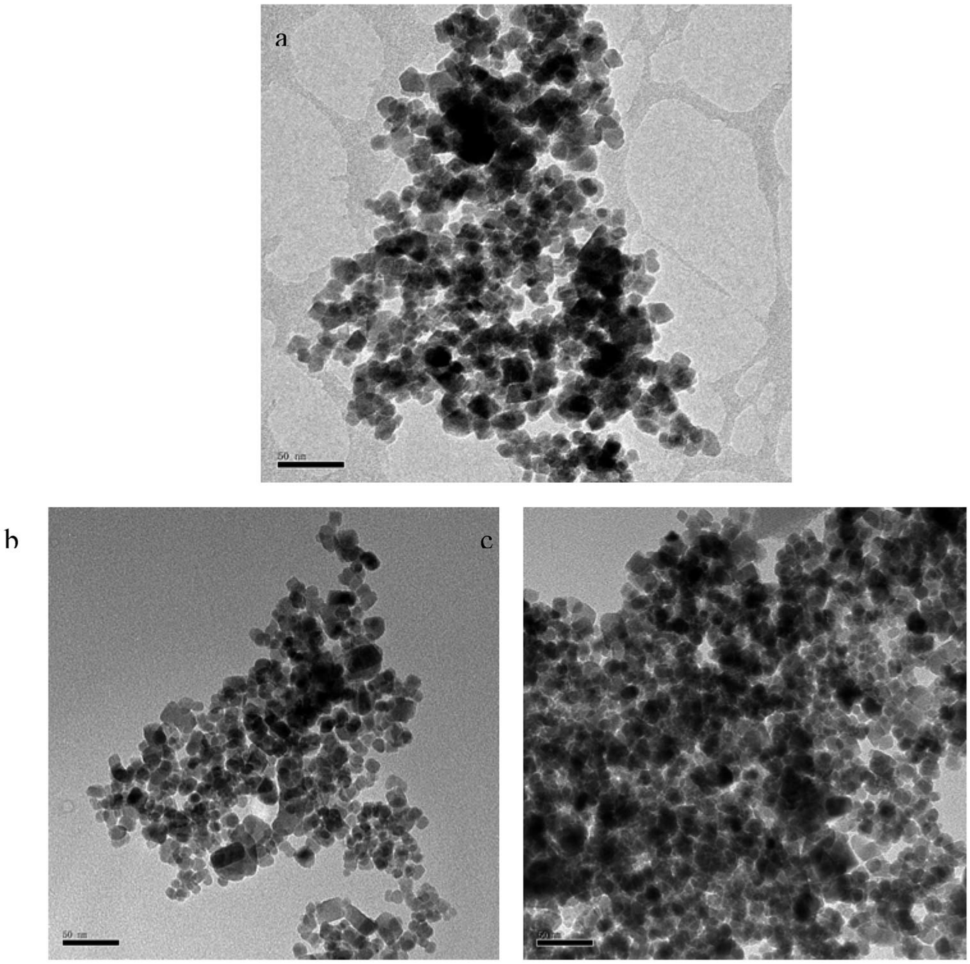

Fig. 3 TEM images of (a) Fe_3O_4 nanoparticles, FePc/Fe_3O_4 nanocomposite (b) before photooxidation and (c) after three times use for photooxidation.

Photocatalytic activity of FePc/Fe_3O_4 nanocomposite

The FePc/Fe_3O_4 nanocomposite was used as the photocatalyst to study the photooxidation of MB in aqueous solution in our work. The spectral changes of MB (10 mg/l) solution in the presence of FePc/Fe_3O_4 nanocomposite and H_2O_2 with visible light irradiation were shown in Fig. 4. The strong absorption peak at 664 and 609 nm is attributed to the monomer absorption and the dimer absorption maximum of MB in aqueous solution, respectively [32]. Figure 4 illustrates that the original peak at 664 nm gradually decreases in 210 min, and no new peaks were observed after the photocatalytic reaction. Due to the photocatalytic degradation products of MB by MPc may be H_2O, NO_3^-, SO_4^{2-}, and NH_4^+ [33], which have no absorption in the range of 400~800 nm. So we can conclude that MB was oxidative degraded by FePc/Fe_3O_4 in the presence of H_2O_2 under visible light irradiation ($\lambda > 420$ nm).

Control experiments of MB (10 mg/l) oxidation under different conditions are illustrated in Fig. 5. It shows that without adding the catalysts, the efficiency of degradation was very low and only 8.1 % MB was oxidized under visible light irradiation (Fig. 5a). In contrast to the solution adding catalysts and H_2O_2 (Fig. 5d), it was clear that adding H_2O_2 can improve the efficiency of photooxidation of MB to a certain extent. After 2 h irradiation, about 78 % MB can be oxidized. In the other hand, the results

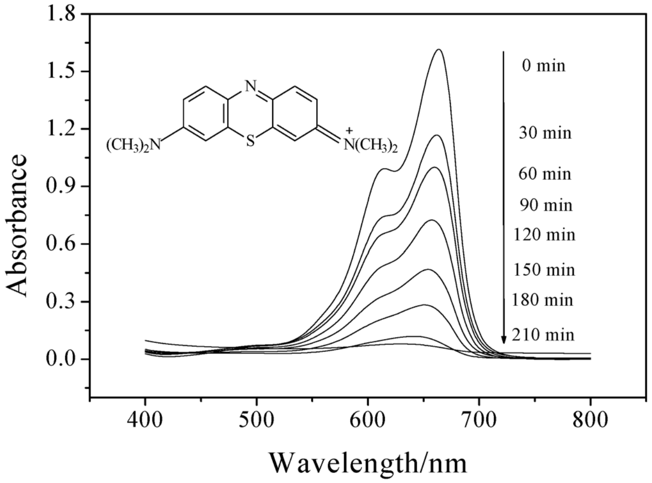

Fig. 4 Absorption spectral changes of 10 mg/l MB aqueous solution as a function of irradiation time ($\lambda > 420$ nm).

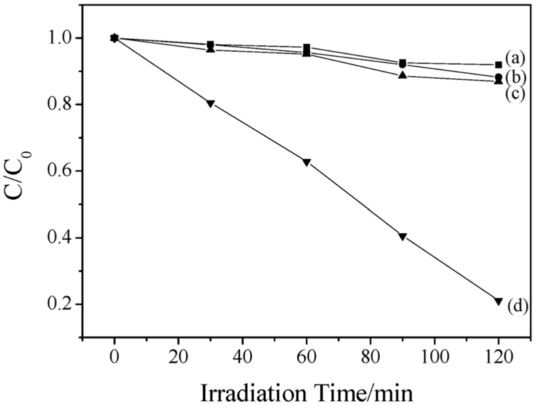

Fig. 5 Degradation of MB with different conditions under visible light: (a) in the absence of catalyst and H_2O_2; (b) with H_2O_2, in the absence of catalyst; (c) in the presence of Fe_3O_4 nanoparticles and H_2O_2; (d) in the presence of FePc/Fe_3O_4 nanocomposite and H_2O_2.

indicated that this functionalized magnetic nanocomposite was active in the photocatalytic oxidation of MB. Additionally, the effects of H_2O_2 and Fe_3O_4 in this system were also investigated. It has already been proved that H_2O_2 has quiet high activity in photocatalytic oxidation under UV light irradiation [34]. However, due to the low yield of active radicals $^{\bullet}$OH under visible light irradiation, only 12 % MB was oxidized, which manifested that H_2O_2 had a negligible impact on the oxidation of MB (Fig. 5b) in this system. It has been proved that Fe_3O_4 nanoparticles as one magnetic support material had small activity with H_2O_2 in the oxidation of MB in our work, which was consistent with the results of Moura's group [35]. As a consequence, it is indicated that Fe_3O_4 nanoparticles only played a supporting role in this composite during the oxidation of MB under visible light irradiation. All the results shown above manifest that the FePc/Fe_3O_4 nanocomposite is photocatalytically active in the oxidation of MB and the efficiency can be greatly improved with the H_2O_2 in this system.

In addition, the effect of the catalyst dosage was investigated in the range of 0~4 g/l. The catalytic efficiency was gradually increased with increasing the dosage of catalyst firstly, and then reaches a plateau from 1 to 4 g/l. Therefore, 1 g/l was selected for further studies.

Effects of the concentration of H_2O_2 on the oxidation efficiency

During our work, it has been proved that H_2O_2 plays an important role in this system, that only less than 5 % MB was photooxidized by the FePc/Fe_3O_4 nanocomposite alone, whereas the efficiency was significantly improved after adding the required amount of H_2O_2. Furthermore, with the optimum condition of the system, the effect of the concentration of H_2O_2 was also discussed with 5 mg/l MB in the presence of 1 g/l catalyst with 2 h irradiation, Table 1. It can be concluded that when the concentration of H_2O_2 increased, the efficiency of photooxidation of MB was also enhanced simultaneously. An explanation is that yields of reactive species $^\bullet$OH photoinduced by FePc/Fe_3O_4 nanocomposite under visible light irradiation are increased when the concentration of H_2O_2 is correspondingly increased. The possible reaction route in which FePc participated in a photo-Fenton-type reaction [15] may be described as follows: the reactive species $^\bullet$OH for the oxidation of MB was generated from H_2O_2 which was excited by the FePc component under visible light irradiation. FePc photoinduces the oxidation of H_2O_2 to produced $HO_2^\bullet$, whereas the reduced MPc Fe(II)Pc is oxidized by H_2O_2 via a dark process to generate $^\bullet$OH [36], eqs. 1 and 2.

$$\mathrm{Fe^{III}Pc + H_2O_2 \xrightarrow{h\nu} Fe^{II}Pc + HO_2^\bullet + H^+} \tag{1}$$

$$\mathrm{Fe^{II}Pc + H_2O_2 \longrightarrow Fe^{III}Pc + {}^\bullet OH + OH^-} \tag{2}$$

Table 1 Effects of the concentration of H_2O_2 on the oxidation efficiency.

$C_{H_2O_2}$ (mol/l)*	C/C_0
3.6×10^{-3}	0.842
1.8×10^{-2}	0.625
5.4×10^{-2}	0.492
9.0×10^{-2}	0.415
1.8×10^{-1}	0.079

*$C_{H_2O_2}$ is the concentration of added H_2O_2 in the reaction system.

Repetitive use of FePc/Fe_3O_4 nanocomposite

After FePc was anchored onto the surface of Fe_3O_4 nanoparticles, which not only kept the magnetism, but also showed excellent photocatalytic activity. During our study, this magnetic composite can be easily recycled using an NdFeB strong magnet. The work was carried out with MB (5 mg/l) with the magnetic nanocomposite (1 g/l) and 1 ml H_2O_2 under visible light for 120 min each time, and it was continually used five times. The activity of this composite was shown in Fig. 6, which manifested that after three times continual utilization, the activity of this catalyst was decreased slowly, however, it still kept its photocatalytic activity after five times. The result may be due to the loss of catalyst when it was recovered and the decomposition of the dye FePc itself with the long time of irradiation in this system [37].

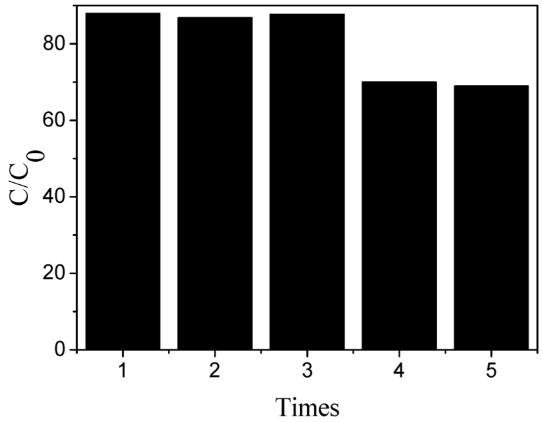

Fig. 6 Effects of repetitive use of the catalyst FePc/Fe_3O_4.

CONCLUSIONS

In summary, we have selected iron(III) phthalocyanine as the model compound of MPcs, and fabricated the core-shell FePc/Fe_3O_4 magnetic nanocomposite by the organic–inorganic complex technique, which provides a promising strategy for preparing magnetically separable photocatalysts in the visible region. The prepared nanocomposites not only prevent the oxidation of Fe_3O_4, but also exert the high photocatalytic activity of FePc for the degradation of organic model dye in the visible region. More importantly, we can separate the fabricated catalyst easily from the solution by using an external magnetic field. After five times continual utilization, this catalyst still kept high photocatalytic activity. With research developments, these functional nanocomposites, MPcs shell/magnetic core, would be extensively applied in the areas of photocatalytic degradation of organic pollutants.

ACKNOWLEDGMENTS

The present work is supported by the National Natural Science Foundation of China (Grant No. 20875039), the Scientific Research Foundation of Jiangsu University (Grant No. 06JDG016), the Research Foundation of Zhenjiang Science and Technology Bureau (Grant No. GY2006021), and Key Laboratory of Analytical Chemistry for Life Science (Grant No. KLACLS07004).

REFERENCES

1. D. Bahnemann. *Sol. Energy* **77**, 445 (2004).
2. J. C. Zhao, C. C. Chen, W. H. Ma. *Top. Catal.* **35**, 269 (2005).
3. U. I. Gaya, A. H. Abdullah. *J. Photochem. Photobiol., C* **9**, 1 (2008).
4. M. R. Hoffmann, S. T. Martin, W. Choi. *Chem. Rev*. **69**, 95 (1995).
5. D. W. Elliott, W. Zhang. *Environ. Sci. Technol.* **35**, 4922 (2001).
6. Z. Li, L. Wei, M. Y. Gao, H. Lei. *Adv. Mater.* **17**, 1001 (2005).
7. V. Augugliaro, M. Litter, L. Palmisano, J. Soria. *J. Photochem. Photobiol., C* **7**, 127 (2006).
8. D. Robert. *Catal. Today* **122**, 20 (2007).
9. G. Wu, A. Chen. *J. Photochem. Photobiol., A* **195**, 47 (2008).
10. M. Alvaro, E. Carbonell, M. Esplá, H. Garcia. *Appl. Catal. B* **57**, 37 (2005).
11. D. Dini, M. Hanack. *J. Porphyrins Phthalocyanines* **8**, 915 (2004).
12. M. Bouvet. *Anal. Bioanal. Chem.* **384**, 366 (2006).
13. C. G. Claessens, U. Hahn, T. Torres. *Chem. Rec.* **8**, 75 (2008).

14. M. Hu, Y. Xu, Z. Xiong. *Chem. Lett.* **33**, 1092 (2004).
15. X. Tao, W. Ma, T. Zhang, J. Zhao. *Chem.—Eur. J.* **8**, 1321 (2002).
16. N. Sehlotho, T. Nyokong. *J. Mol. Catal. A* **219**, 201 (2004).
17. K. M. Parida, N. Baliarsingh, B. Sairam Patra, J. Das. *J. Mol. Catal. A* **267**, 202 (2007).
18. W. X. Chen, W. Y. Lu, Y. Y. Yao, M. H. Xu. *Environ. Sci. Technol.* **41**, 6240 (2007).
19. X. Zhao, Z. Li, Y. Chen, L. Shi, Y. Zhu. *Appl. Surf. Sci.* **254**, 1825 (2008).
20. V. Iliev, D. Tomova. *Catal. Commun.* **3**, 287 (2002).
21. V. Iliev, D. Tomova, L. Bilyarska, L. Prahov, L. Petrov. *J. Photochem. Photobiol., A* **159**, 281(2003).
22. S. Rana, J. Rawat, R. D. K. Misra. *Acta Biomater.* **1**, 691 (2005).
23. J. Rawat, S. Rana, R. Srivastava, R. D. K. Misra. *Mater. Sci. Eng., C* **27**, 540 (2007).
24. Y. Gao, B. H. Chen, H. L. Li, Y. X. Ma. *Mater. Chem. Phys.* **80**, 384 (2003).
25. W. L. Kostedt, J. Drwiega, D. W. Mazyck, S. W. Lee, W. Sigmund, C. Y. Wu, P. Chadik. *Environ. Sci. Technol.* **39**, 8052 (2005).
26. E. A. Reyes-Garcia, Y. P. Sun, D. Raftery. *J. Phys. Chem. C* **111**, 17146 (2007).
27. Y. H. Ao, J. J. Xu, D. G. Fu, X. W. Shen, C. W. Yuan. *Sep. Purif. Technol.* **61**, 436 (2008).
28. K. T. Wu, P. C. Kuo, Y. D. Yao, E. H. Tsai. *IEEE Trans. Magn.* **37**, 2651 (2001).
29. R. Y. Hong, B. Feng, Z. Q. Ren, B. Xu, H. Z. Li, Y. Zheng, D. G. Wei. *Chem. Eng. J.* **144**, 329 (2008).
30. G. Sivalingam, K. Nagaveni, M. S. Hegde, G. Madras. *Appl. Catal. B* **45**, 23 (2003).
31. R. M. Mohamed, M. M. Mohamed. *Appl. Catal. A* **340**, 16 (2008).
32. T. Zhang, T. Oyama, S. Horikoshia, H. Hidaka, J. Zhao, N. Serpone. *Sol. Energy Mater. Sol. Cells* **73**, 287 (2002).
33. K. M. Parida, N. Baliarsingh, B. Sairam Patra, J. Das. *J. Mol. Catal. A* **267**, 202 (2007).
34. F. Banat, S. A1-Asheh, M. A1-Rawashdeh, M. Nusair. *Desalination* **181**, 225 (2005).
35. F. Moura, M. H. Araujo, R. Costa, J. Ardisson, W. Macedo, R. M. Lago. *Chemosphere* **60**, 1118 (2005).
36. K. T. Ranjit, I. Willner, S. Bossmann, A. Braun. *J. Phys. Chem. B* **102**, 9397 (1998).
37. H. Shu, M. Chang. *J. Hazard. Mater. B* **125**, 96 (2005).